ORIGINAL ARTICLE

Enhancement of the bond behaviour between sand coated GFRP bar and normal concrete using innovative composite anchor heads

Milad Shakiba · Seyed Mohammad Hosseini · Milad Bazli [ORCID] · Seyed Mohammad Reza Mortazavi · Mohammad Ali Ghobeishavi

Abstract Anchor heads could efficiently address the bond weakness between Fibre-Reinforced Polymer bars and concrete. This experimental study enhanced the bond behaviour between GFRP bars and concrete using three innovative anchorage systems made from glass fibre cloth and epoxy resin. A direct pullout test was used to study the bond-slip performance between the bar and the concrete. Test variables were GFRP bar diameter (3 diameters), concrete compressive strength (20.4 and 40.2 MPa), and anchor system (three different types). Based on the test results, in low-strength concrete (i.e. 20.4 MPa) samples, the anchor system efficiency was not promising, and the failure occurred between the concrete and anchors. However, for higher strength concrete (i.e. 40.2 MPa) samples, the ultimate developed tensile load increased between 14 and 68% for different bar sizes and anchorage systems compared to the unanchored control specimens.

M. Shakiba · S. M. Hosseini · S. M. R. Mortazavi · M. A. Ghobeishavi
Department of Civil Engineering, Shahid Rajaee Teacher Training University, Lavizan, Tehran, Iran

M. Bazli (✉)
College of Engineering, IT & Environment, Charles Darwin University, Darwin 0801, Australia
e-mail: milad.bazli@cdu.edu.au; m.bazli@uq.edu.au

M. Bazli
School of Mechanical and Mining Engineering, The University of Queensland, Brisbane, Australia

1 Introduction

Corrosion is a major contributor to steel-reinforced concrete members' degradation and structural deficiency. This issue is amplified in severe environments where steel corrosion could make structures vulnerable and necessitate costly rehabilitation and repair. Corrosion of reinforcing steel bars causes a loss of serviceability or strength capacity in such structures [1, 2]. Various techniques, such as replacing damaged concrete and using non-steel, stainless steel, or galvanized steel components, have been investigated by researchers in the past to address this issue. Apart from their benefits, they are relatively expensive and have certain performance downsides, such as low shear strength, brittle failure, and vulnerability to fire and the alkaline environment, particularly in the long run. Fibre-reinforced polymer (FRP) bars with non-corrosive properties and relatively high strength/stiffness-to-weight ratio compared with steel have been offered as an alternative to carbon steel bars [3, 4]. Using FRP as reinforcement in various applications could be cost-effective and help has environmental benefits while also extending the structure's service life [5–7]. Corrosive resistance, lightweight, high tensile strength, and electric insulation are benefits of FRP

reinforcing bars over steel, making them ideal materials to solve durability challenges associated with steel reinforcing bars [5, 8–10]. FRP bars have recently been used to reinforce and strengthen various concrete structures subjected to harsh environmental conditions. For example, marine constructions, pipelines, and bridge decks are some of such applications [11]. Magnetic resonance imaging facilities, electrical substations, boring tunnel activities, and traffic barriers have all used FRP bars in the past [12, 13]. Glass FRP (GFRP) bars have received greater attention than other FRP forms, owing to their lower cost [8]. Admittedly, widespread acceptance of GFRP bars for structural applications, particularly in harsh environments, appears to be on hold at the moment, potentially due to a lack of validated and reliable data on the use of GFRP in harsh environments such as the marine environment, and high alkalinity solutions [12, 14, 15]. As a result, it is critical to understand the behaviour of GFRP-reinforced concrete members under various loads and environmental conditions [3]. Accordingly, the bonding mechanism between GFRP bars and concrete is one of the most important elements, particularly in a harsh environment [11].

Straight bars with inappropriate development length are dangerous in concrete structures. The design moments and forces will not be reached in structural members if the necessary bond development length is not provided in bars, which may lead to structure failure [16–18]. Bond stresses transferred between the reinforcing bars and the surrounding concrete generally depend on the quality of the bond. Regardless of the type of bars, the load transfer mechanism and bond length are critical issues in structural design. [19–21]. Load transfer mechanism and development length of steel and FRP bars are affected by a number of factors, including concrete type, bar type and diameter, mechanical properties and surface configuration of FRP bars [22]. Generally, the load is transferred between the concrete and FRP bar through the chemical bonds, friction, and mechanical interlocking [23–25].

There have been a few investigations on the bond performance of FRP bars embedded in concrete. Cosenza [26], for example, investigated the bond stress-slip behaviour of concrete and FRP bars and proposed changes to computational models' bond prediction evaluation. Hasaballa et al. [27] studied the seismic behaviour of GFRP-reinforced beam columns,

and their findings revealed that straight bars perform better than bent bars. The bond properties of various GFRP reinforcements were examined, and the effect of FRP bar dimensions and properties on the bond stresses was identified. Mohamed and Benmokrane [28] investigated the pullout performance of FRP bars embedded in concrete and discovered the efficiency of using FRP bars as an alternative to steel reinforcement.

However, several of the drawbacks of FRP reinforcement limit its widespread application. Anchoring bars with insufficient embedding lengths are a serious challenge in FRP-reinforced elements. Using regular $90°$ and $180°$ bends in the bars is a common solution in steel-reinforced elements. However, FRP bars cannot be bent once manufactured, and if they are made with hooks, the redirection of the fibre at the curved part reduces their strength significantly [29]. For the issue of load transfer between concrete and FRP bars, anchor plates and heads may be a preferable option.

In an experimental study by Shakiba et al. [30], the effect of glass fibre mat anchorage on the pullout behaviour of sand-coated GFRP bars embedded in normal strength concrete was investigated. The results of their study demonstrated that by reducing concrete strength, the effect of the anchorage system on the bond behaviour of GFRP bars decreases. Their study was the extension of the same anchorage system proposed by Ashrafi et al. [31]. The proposed system's effectiveness was evaluated using the direct pull-out test.

Elsayed et al. [32] investigated the performance of FRP-bar reinforced concrete beams with composite anchorages constructed of steel tubes filled with high-performance resins embedded along the bars. Steel tubes provide a good stress transmission between FRP bars and concrete when used as an anchoring system. According to their findings, increasing the number of anchorages along with FRP bars improves the ultimate load compared to the straight bar.

The influence of headed-end bars on the pullout strength of GFRP bars in high-strength concretes was investigated by Islam et al. [19]. For the various cases, their findings revealed that bond length and pullout force increased in samples with a headed-end bar compared to samples with a straight bar. Variables, including bars diameter, development lengths (4 or 6 times the bar diameter), anchors, and concrete cover

values, were investigated in their research. Khed-erzadeh and Sennah [33] evaluated 114 pull-out specimens reinforced with GFRP bars and found that headed GFRP bars have a greater anchoring capacity than hooked bars. Maranan et al. [34] investigated the influence of head anchors on the pullout behaviour of sand-coated GFRP in geo-polymer concrete. The use of head anchors increased the anchorage capacity by 49–77%, according to their findings. Benmokrane et al. [35] investigated the physical and durability characteristics of innovative headed GFRP bars for concrete structures. The influence of confinement, bar diameter, concrete compressive strength, and exposure conditions on the pullout behaviour of headed GFRP bars was investigated. According to their findings, the head's geometry, interface, and config-uration can result in proper mechanical interlocking for the GFRP bars. Up to 63% of the guaranteed tensile strength of straight GFRP bars was attained for 15.9 and 19 mm diameter bars with head ends, respectively. Additional aluminium alloy ribs anchoring was employed by Zhang et al. [36] to improve the bond behaviour of CFRP bars tested in the pullout. As expected, the development length of CFRP bars was reduced by using additional ribs (AR) anchoring.

Despite efforts to improve the bond between FRP bars and concrete, there is still a long way to go in ensuring proper bond performance in FRP-reinforced concrete structures. To overcome some of the chal-lenges associated with the current anchorage systems, such as manufacturing and applying complexities. The present study offers a simple, efficient and cost-effective anchorage system for FRP reinforcing bars in order to reach the FRP bars' ultimate tensile strength when used as internal reinforcements for reinforced concrete structures. In support of this endeavour, new forms of glass-fibre anchor heads for GFRP bars were investigated in the current study. 72-pullout specimens were tested to see how the proposed anchor head, concrete compressive strength, and bar diameter affect the bond behaviour between GFRP bars and concrete. Furthermore, the load-slip relationship, failure mech-anism, and tensile stress developed in GFRP bars are presented in detail. Given the results obtained, if adequate concrete compressive strength is provided, the developed tensile stress in the FRP bar can be improved by up to 68%, depending on the bar size and anchorage type.

2 Experimental program

Material properties, specimen preparation and char-acteristics, and pullout test methodology are explained in this section.

2.1 Material properties

2.1.1 GFRP bars

Sand-coated GFRP bars used in this study were made of 65% E-glass fibre and 35% epoxy resin by volume. Three bar diameters with effective cross sections of 31.7, 71.3, and 126.7 mm^2 were used. In order to obtain the mechanical properties of GFRP bars, three identical samples were tested according to ASTM D7205/7205M21 [37], and the average results were used for discussion and comparison (Table 1).

2.1.2 Concrete

Two types of concrete were considered, namely C1 and C2, produced using general purpose Portland cement (Type II Portland cement, whose specific surface was 3050 cm^2/gr, and its chemical specifica-tions are presented in Table 2). The initial concrete mix and fresh properties were designed based on ACI 211 [38]. After 28 days, six cylindrical 150 × 300 mm specimens were examined to obtain the concrete compressive properties according to ASTM C39 / C39M [39]. The mixed proportion of concretes and slump test results are shown in Table 3. The average compressive strength obtained for the concrete types C1 and C2 were 20.4 ± 1.1 MPa and 40.2 ± 2.3 MPa for 28 days, respectively.

2.1.3 Anchor head

The materials used to fabricate the anchorage systems used in this study were glass fibre cloth and epoxy resin. In order to increase the internal bond strength between the GFRP bars and the anchorage, the inner side of the anchors was grooved. Epoxy resin was used to fill the gap between the bar and the anchor. The length of the proposed anchor head was selected as 80 mm and constant for all specimens. The anchor head's outer diameter is selected to be approximately three times the diameter of the bar. The geometric characteristics of the proposed anchor are presented in

Table 1 Geometrical and mechanical properties of the GFRP bars

Bar diameter (mm)	Cross section area (mm^2)	Tensile strength f_{ps} (MPa)	Modulus of elasticity (GPa)	Poisson's ratio
6.35 (#2)	31.7	990 ± 23	51 ± 4.8	0.25
9.52 (#3)	71.3	1100 ± 51	49.5 ± 4.1	0.21
12.7 (#4)	126.7	1140 ± 36	51.2 ± 2.6	0.26

Numbers in the () are the manufacturer's bar designation

Table 2 Physical and chemical properties of the cement

Material	Chemical analysis (%)									Specific surface (cm^2/gr)
	SiO_2	Al_2O_3	Fe_2O_3	CaO	MgO	SO_3	Na_2O	K_2O	L.O.I	
Cement	21.8	4.85	3.53	63.43	1.52	2.13	0.36	0.56	2.4	3050

Table 3 Mix proportion of concretes

| Type	Water-cement ratio	Water (kg/m^3)	Cement (kg/m^3)	Gravel 4–20 mm (kg/m^3)	Sand 0–4 mm (kg/m^3)	Slump (mm)
C1	0.5	200	400	900	800	85
C2	0.405	162	400	850	840	75

Table 4 Properties of proposed anchor heads

Anchor type	Bar	First diameter of anchor head (mm)	Second diameter of anchor head (mm)	Third diameter of anchor head (mm)	Forth diameter of the anchor head (mm)
II	(#2)	19	19	–	–
	(#3)	28	28		
	(#4)	38	38		
III	(#2)	19	19	10	–
	(#3)	28	28	14	
	(#4)	38	38	19	
IV	(#2)	19	19	12	9
	(#3)	28	28	18	12
	(#4)	38	38	25	16

Table 4 for each corresponding bar diameter. Three different cross sections were considered anchor systems. In fact, the effects of the shape and variations of the anchor cross-section along the anchor head have been investigated to study how the stress is distributed and transferred from the bar to the concrete. It should be noted that the largest anchor diameter remained constant among all anchor types. Figure 1 illustrates GFRP bars with anchor heads.
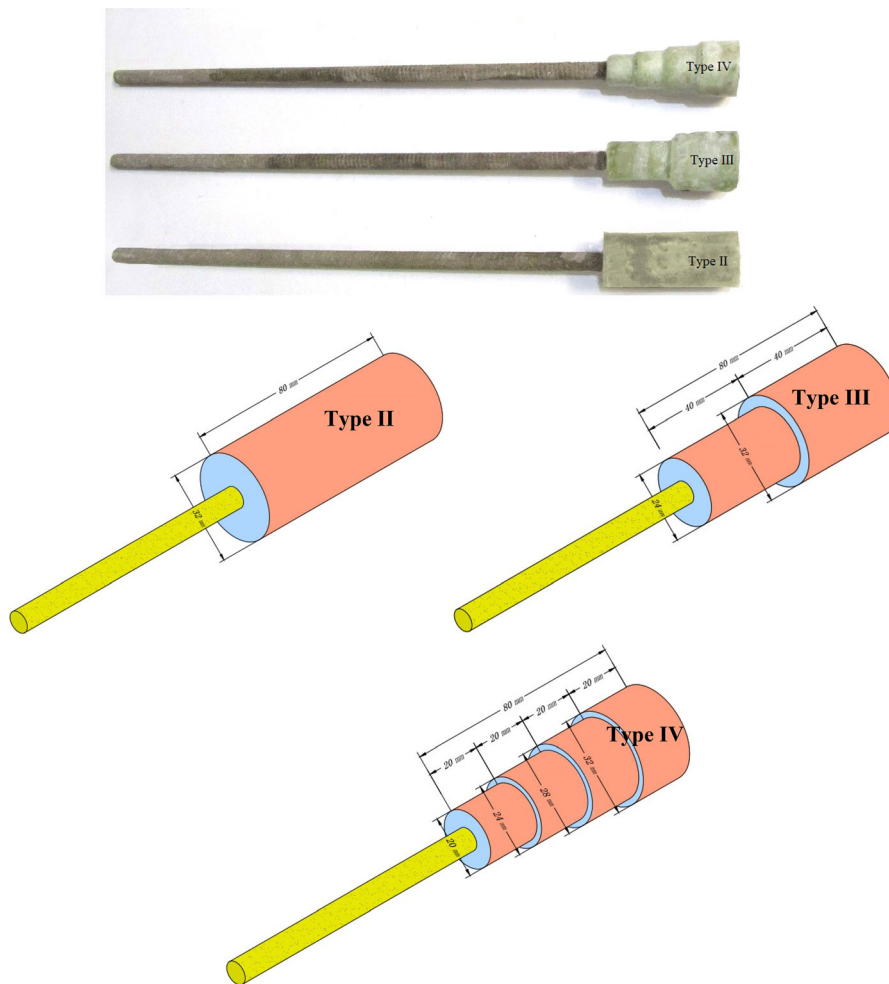
Fig. 1 GFRP bars with different types of proposed anchor heads

2.2 Specimens configuration

In this research, three different shapes of anchor heads were tested to enhance the bond behaviour between the sand-coated GFRP bar and concrete. Figure 2 shows the configurations of the specimens according to the various types of anchor heads. Type I specimens were without anchor and were considered as the reference samples. As seen in Fig. 2 and Table 4, the specimens with anchors are categorized into three groups, i.e. II, III, and IV. Each specimen has been labelled and identified according to the type of concrete, the shape of the anchor head, and the diameter of the bars used. For instance, specimen C2-SII-D2 is identified as follows: C2 is the concrete specification (concrete with compressive strength of 40.2 MPa), SII is the shape of the proposed anchor head (anchor type II), and D2 represents the GFRP bar diameter (manufacturer's bar designation). All pull-out specimens were tested after 28 days of construction.

As seen in Fig. 2, the total bond length between GFRP bars and concrete differs among different specimen types. As a result, the direct comparison of the bond strength between different types will not be realistic. Therefore, in order to appropriately compare the pull-out performance of different types, in the present study, the behaviour of the specimens under pull-out loading is determined by the tensile stress (f_s) developed in the GFRP bar. Tensile stress in GFRP bars is obtained by dividing the pull-out load applied to the nominal cross-section of the bar.
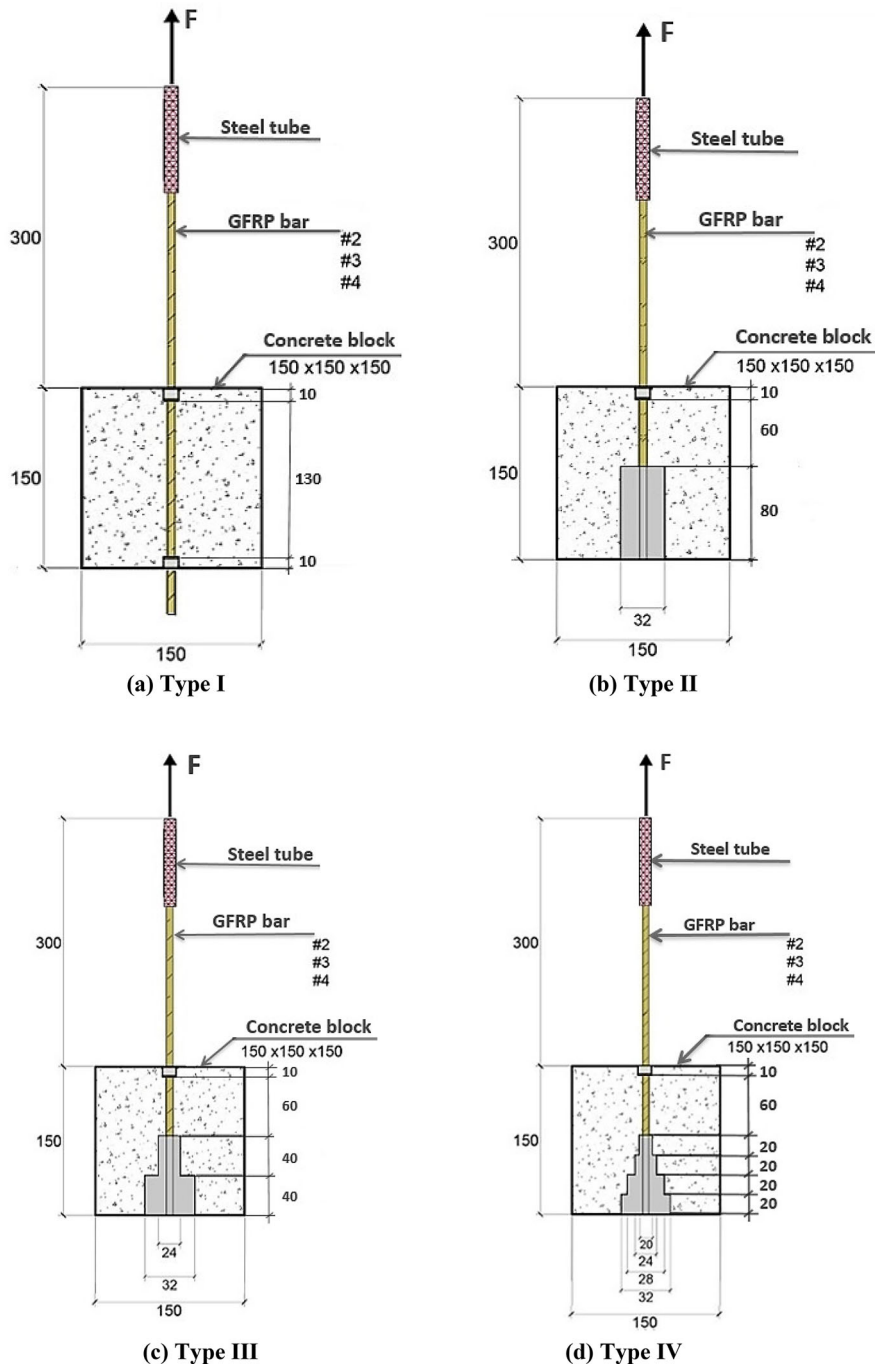
(a) Type I

(b) Type II

(c) Type III

(d) Type IV

Fig. 2 Specimen parameters

2.3 Direct pullout test

In order to conduct the direct pullout test, a UTM Zwick Roell test machine with a capacity of 150kN has been used. To achieve the full range behaviour of the specimens during the test, a 1.2 mm/min loading rate was used under displacement-control mode. A steel frame was manufactured to transfer the load

applied by the machine to the specimen. Two LVDTs were positioned at the un-loaded free end and loaded end of the bar. The recordings of the bottom LVDT (un-loaded end) were used to obtain the bar slip values, while the recordings of the top LVDT (loaded end) were used to obtain the total displacement of the specimen. Figure 3 illustrates the schematic drawing and actual pullout test set-up used. According to the CSA: S806-12 [40], the testing process continues until the time when one of the following failure modes occurs: (i) Cracking and crashing of the surrounding concrete; (ii) Approximately 5 mm bar slip; (iii) Failure of the FRP bar or the anchor head.

3 Experimental results

In this section, the results of experimental tests, such as load-slip relationship, bar tensile stress, and failure modes of specimens, are presented and discussed in detail. The effects of various factors, such as the anchor shapes, concrete compressive strength and

GFRP bar diameter, on bond performance, were investigated.

3.1 Failure modes

The effect of various parameters on the failure mode of specimens is discussed in this section. Typical failure modes observed during pullout tests are shown in Fig. 4. These failure modes are as follows:

(i) Pullout failure (PF) (Fig. 4-a): in this type of failure, the GFRP bar is pulled out from the inside of the concrete block without any progressive concrete cracking. The pull-out type of failure occurred when the confining strength of the concrete cube was less than the radial splitting stress produced by the bond between the bar and the concrete. This shows that the concrete shear strength and concrete block confinement strength were adequate so that no interfacial crack was propagated toward the concrete surface. This mode of failure was generally found in specimens without anchors.
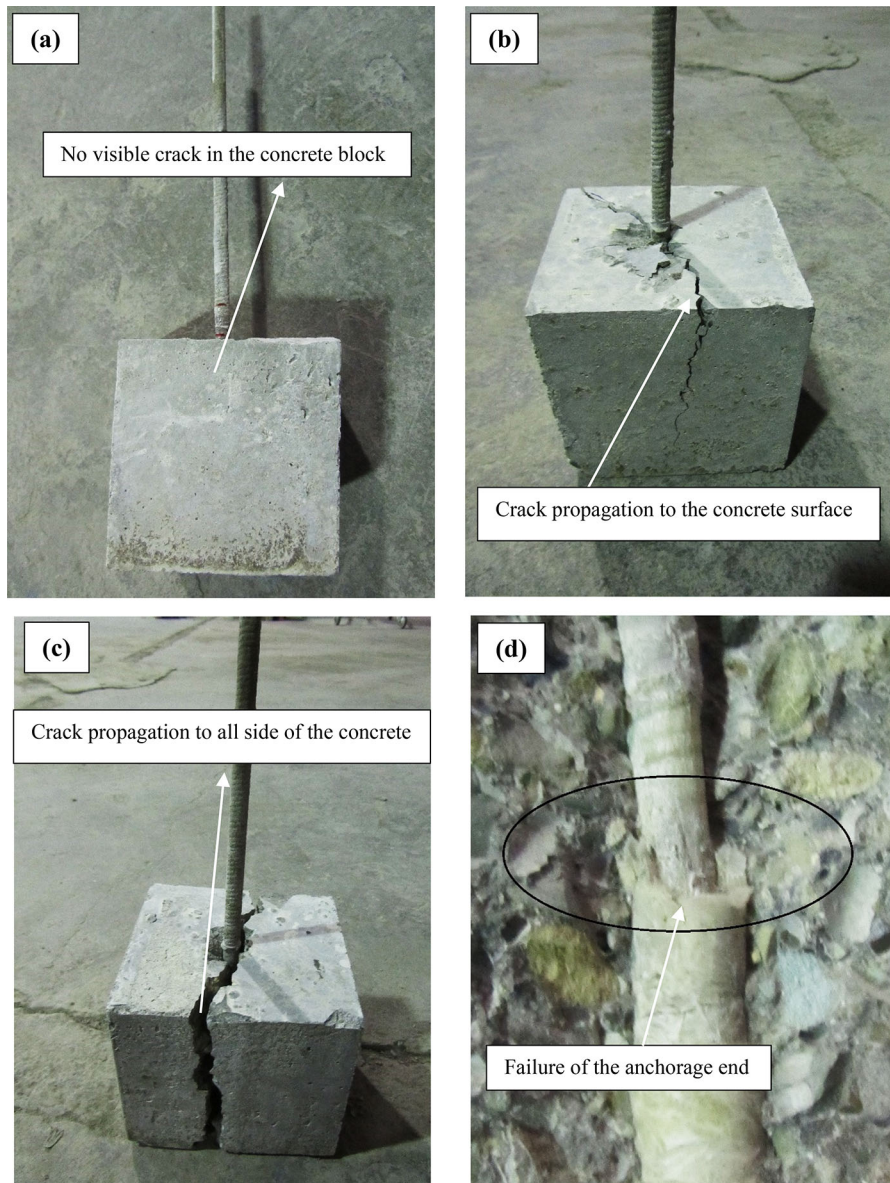

(a) Actual set-up
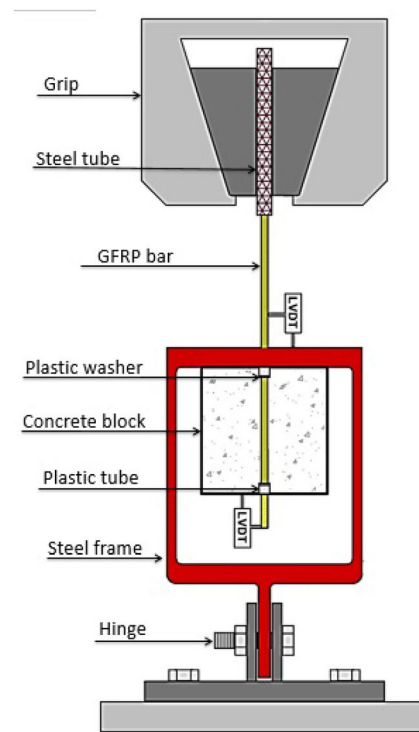
(b) Schematic

Fig. 3 Test set-up

Fig. 4 Typical modes of failures observed: **a** Pullout failure (PF); **b** Partial concrete splitting (PCS); **c** Full concrete splitting (FCS); **d** Anchor head failure (AHF)

(ii) Partial concrete splitting (PCS) (Fig. 4-b): in this mode, a crack is occurred on the concrete surface, leading to a partial splitting failure in the concrete block. The concrete splitting occurred as the hoop tension became more than the shear capacity of the concrete, causing wider longitudinal cracks and their propagation to the external surface. This failure mode is observed in specimens with anchors type II and III in both types of concretes with different bar diameters. In

addition, specimens with Type III anchors showed wider cracks than specimens with other anchor types. Due to the extra bearing resistance of the anchor head, which resulted in a substantial portion of radial splitting stress in the concrete, the failure mode of GFRP bars with headed anchors embedded in concrete changed from bar pull-out to concrete splitting. Since splitting failure mode is an unstable mode and depends on several factors, such as concrete tensile strength,

concrete cover, bar and anchor head diameter, and friction in the reaction plate, it is difficult to differentiate the contribution of each resistance mode.

(iv) Full concrete splitting (FCS) (Fig. 4-c): In this mode, the concrete block shows wider cracks due to the higher strength of the anchor system. The initial cracks eventually lead to the total failure of the concrete and the creation of a split at the bar's location and its propagation to the outer surfaces.

Type IV specimens have experienced this failure mode due to the higher mechanical interlocking and frictional stresses along with the anchor compared to the other specimens.

(v) Anchor head failure (AHF) (Fig. 4-d): This mode of failure is due to the proper distribution of stress along with the anchorage system and appropriate mechanical and frictional interaction between the bar, the anchor, and the concrete under pullout loads. In fact, the anchor has shown an appropriate strength due to its proper bonding with the bar and has experienced a failure in the expected area because of stress concentration.

It is worth mentioning that, as expected, none of the samples failed in FRP bar rupture due to the relatively low confinement strength of the concrete for such a strong anchorage system. Also, all three identical samples have shown the same failure modes.

3.2 GFRP bar tensile stress

In order to increase the reliability of the results, three identical samples were tested for each condition, and the average results were used for discussions and conclusions. To quantify the efficiency of using the anchor system and their shapes, the ratio between the developed tensile stress (f_s) and nominal tensile strength of GFRP bars, f_{ps} was calculated. Table 5 summaries the average pullout test results in terms of the maximum load, f_s, f_s / f_{ps} ratio and failure modes. As shown in Table 5, for concrete C2 the presence of anchors increases the developed tensile stress by 14 to 71% compared to specimens without anchors. This indicates that the proposed anchorage system provides adequate mechanical interlocking and increases friction along with the specimen. Furthermore, the efficiency of the anchor significantly reduces in low strength concrete (i.e. 20.4 MPa), where concrete cracking occurs due to low concrete shear strength. As a result, concrete with

suitable compressive strength is required to accomplish the desired efficiency of using the proposed anchor heads.

Figure 5 shows the representative (i.e. one sample was randomly selected out of the three identical specimens) developed bar tensile stress (f_s) versus slip curves of all tested specimens. It should be mentioned that identical samples showed almost the same pullout behaviour.

The slippage of the bar was measured using the LVDT located at the unloaded end of the bar. The test continued until the bond failure occurred. The end of the test was considered when at least a 20% drop of the maximum applied load was reached.

As is seen in Fig. 5, for both concrete types, the bar stress-slip curves showed an ascending branch up to a maximum stress value. Specimens showed a three-stage slip evolution behaviour. The first stage was before the chemical bond breaking in which no slip was recorded. The second stage was from the slip initiation (chemical breaking moment) until the maximum bar stress (ascending stage) and the third stage was from the maximum bar stress until the end of the pull-out test (descending stage). The third stage for most of the samples includes a sudden stress drop.

In anchored specimens with C1 concrete type, the slip starts almost the same or even earlier than the reference sample (i.e. C1-SI samples). As mentioned earlier, early crack development due to the low shear strength of concrete and the high strength/stiffness of the anchorage is the main reason for such early slip initiation. However, despite C1 samples, for anchored specimens with C2 concrete type, the slip starts later than that of specimens without an anchor. This is due to the concrete's high load-carrying capacity and the crack initiation delay. This further confirms the efficiency of the proposed anchorage systems in structures with higher concrete compressive strength.

In addition, in higher-strength concrete samples, anchor heads contribute significantly to load-bearing capacity, while the anchor shapes significantly affect surface cracks, bond stress distribution and splitting stresses. In other words, the earlier slip of specimens without anchor is due to the lesser mechanical interlocking between the concrete and GFRP bar. Moreover, the applied loading is resisted only by the bond between the bar and the concrete. In this case, bond strength is due to the frictional forces and

Table 5 Pullout test results summary

Specimen	P (kN) ± S.D. (kN)	f_s(MPa)	f_s/f_{ps} (%)	Failure mode
C1-SI-D2	14.2 ± 0.5	447.9	45.2	PF
C1-SII-D2	12.5 ± 0.9	394.3	39.8	PCS
C1-SIII-D2	10.7 ± 0.6	337.4	34.1	PCS
C1-SIV-D2	9.1 ± 0.8	287.1	28.9	FCS
C1-SI-D3	32.1 ± 0.3	450.2	40.9	PF
C1-SII-D3	27.2 ± 1.3	381.5	34.7	PCS + PF
C1-SIII-D3	23.9 ± 0.5	335.2	30.5	PCS
C1-SIV-D3	22.2 ± 1.3	311.4	28.3	PCS
C1-SI-D4	42.7 ± 0.7	337.1	29.6	PF
C1-SII-D4	40.4 ± 0.9	318.8	27.9	PCS
C1-SIII-D4	39.3 ± 1.8	310.2	27.2	PCS
C1-SIV-D4	31.7 ± 0.9	250.2	21.9	FCS + AHF
C2-SI-D2	10.8 ± 0.9	340.7	34.4	PF
C2-SII-D2	14.2 ± 0.8	448.0	45.2	PCS
C2-SIII-D2	15.8 ± 1.6	498.4	50.3	PCS + AHF
C2-SIV-D2	16.1 ± 1.7	507.9	51.3	FCS + AHF
C2-SI-D3	20.1 ± 0.9	281.9	25.6	PF
C2-SII-D3	24.1 ± 1.6	338.0	30.7	PCS
C2-SIII-D3	30.4 ± 1.4	426.4	38.7	PCS
C2-SIV-D3	34.5 ± 0.8	483.8	44.9	FCS + AHF
C2-SI-D4	44.2 ± 1.6	348.8	30.6	PCS + PF
C2-SII-D4	46.3 ± 2.8	365.4	32.1	PCS + PF
C2-SIII-D4	59.1 ± 2.8	466.5	40.9	PCS + AHF
C2-SIV-D4	63.5 ± 2.4	501.2	43.9	FCS + AHF

PF Pullout failure; *PCS* Partial concrete splitting; *FCS* Full concrete splitting; *AHF* Anchor head failure

mechanical interlocking between the sand-coated bar and the concrete.

3.3 Load–displacement relationship

This section investigates the load–displacement behaviour between the GFRP bar and concrete. Figure 6 shows the representative (i.e. one sample was randomly selected out of the three identical specimens) pull-out load–displacement curves of all tested specimens. Because of the low compressive strength and, as a result, low shear strength of concrete type C1, it has been observed that the anchor system nearly lowers the specimen stiffness. In other words, due to the low shear strength of the concrete and high strength and stiffness of the anchorage system, the anchor results in crack initiation and propagation in the surrounding concrete and, consequently, stiffness and strength reduction of the specimen. Finally, premature concrete split failure occurs before pullout

failure, which is the main result of the relatively low bond strength of C1 anchored bar specimens compared to the C1 straight bar specimen. However, in C2 concrete type specimens, due to the higher shear strength of the concrete, much higher shear stress and, consequently, higher loads are carried by the concrete. Therefore, due to the higher bearing and friction surface between the anchored bar and the concrete compared to the corresponding straight bar, higher bond loads have been observed for C2 anchored samples compared to the corresponding reference specimen (i.e. straight bar).

As is seen in Fig. 6, the anchor type IV has the highest pullout force because of the larger friction surface and more mechanical interlocking forces generated between the anchor and concrete. In anchored bars with higher strength concrete, longitudinal and surface cracks lead to a decrease in the bond stiffness (i.e. lower slope of the curve after the initial linear section). However, similar to the anchored bars
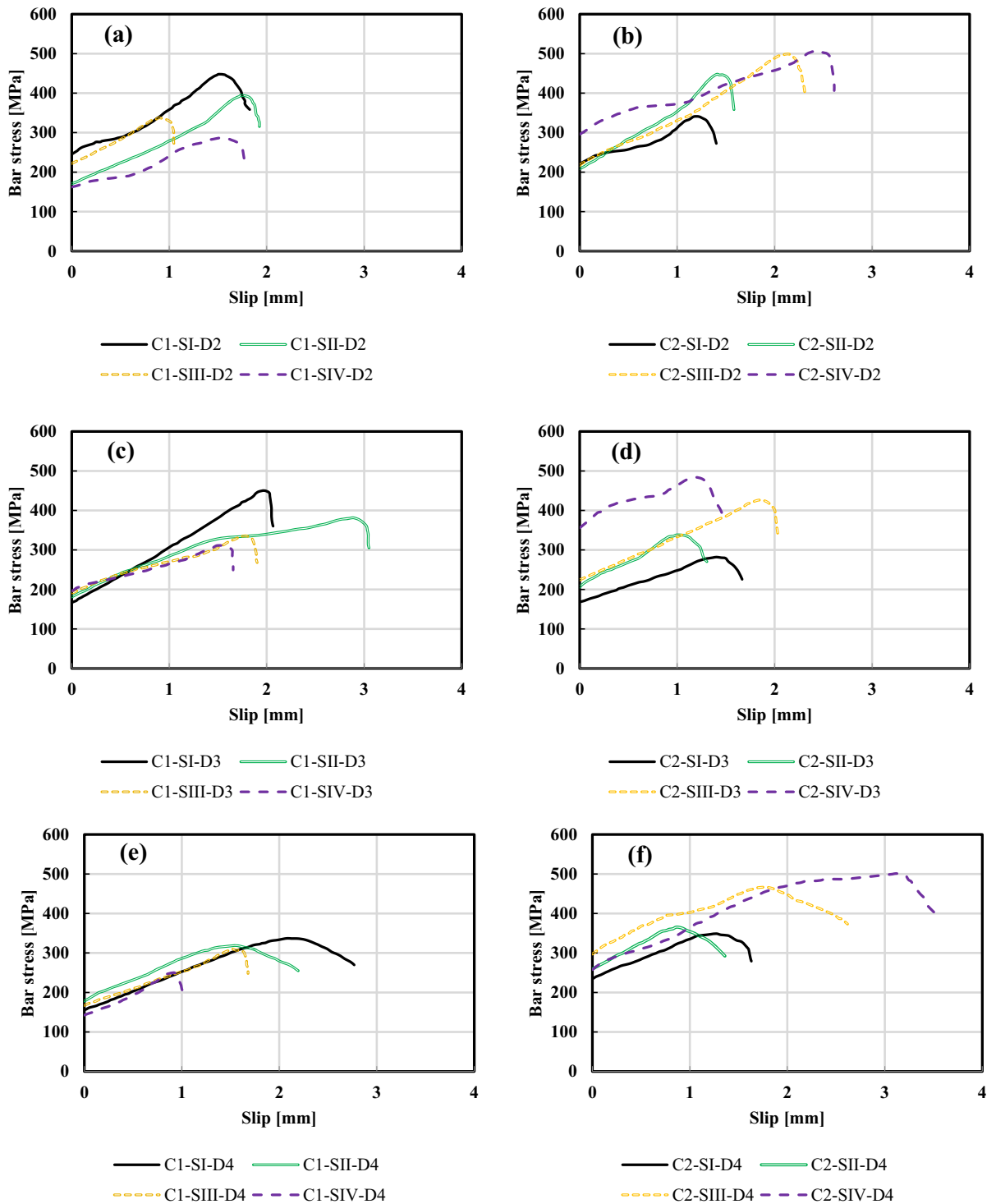
Fig. 5 Bar stress-slip curves: **a** bar #2 and C1 concrete; **b** bar #2 and C2 concrete; **c** bar #3 and C1 concrete; **d** bar #3 and C2 concrete; **e** bar #4 and C1 concrete; **f** bar #4 and C2 concrete
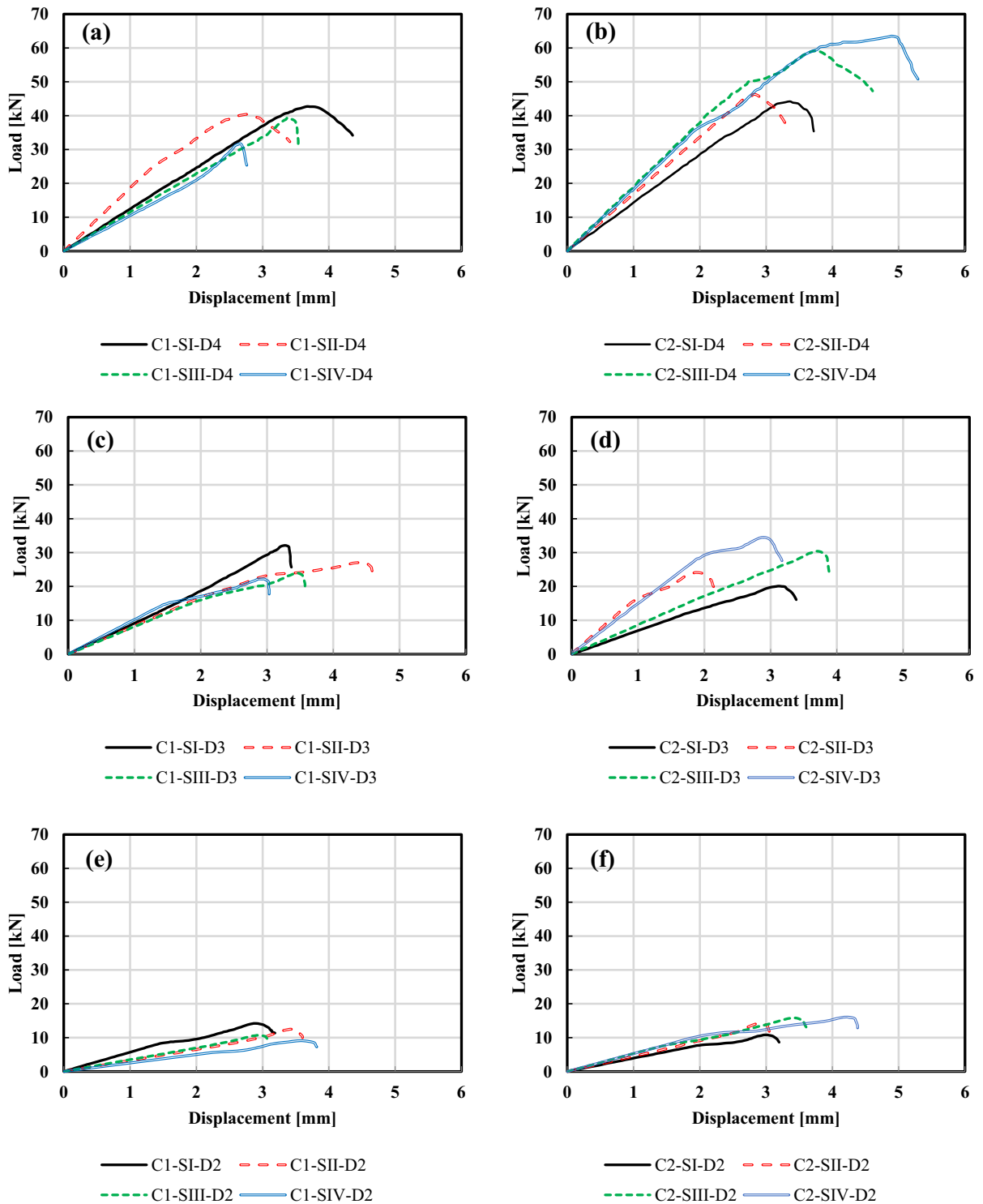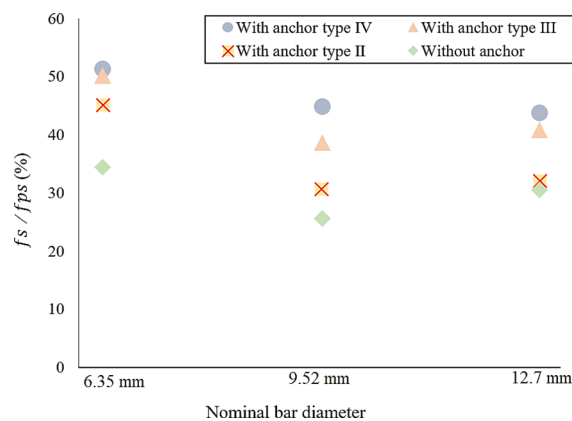
Fig. 6 Load–displacement curves: **a** bar #4 and C1 concrete; **b** bar #4 and C2 concrete; **c** bar #3 and C1 concrete; **d** bar #3 and C2 concrete; **e** bar #2 and C1 concrete; **f** bar #2 and C2 concrete

with lower strength concrete, the failure of the specimens was due to the cracks propagation towards the concrete block surface and eventually concrete splitting (the failure modes will be explained in detail later on). Based on these observations, one could conclude that the innovative proposed anchorage system could be significantly beneficial if an appropriate concrete compressive strength is guaranteed: the higher the compressive strength, the higher the bond strength (until the bar rupture).

3.4 Parametric study

This section investigates the effects of each studied parameter on the specimens' pullout behaviour. These parameters include the GFRP bar diameter, concrete compressive strength, and the shape of the anchor. It is worth mentioning that since the bond length between the un-anchored and anchored specimens was not equal among different specimen types, the developed tensile stress in GFRP bars stress was considered as the output of the ANOVA analysis in this study.

3.4.1 Influence of bar diameter

Generally, the pullout behaviour is affected by the diameter of the GFRP bars. Figure 7 illustrates the effect of the bar diameter on the developed tensile stress ratio in the specimens (f_s/f_{ps}). In most cases, the f_s/f_{ps} ratio decreases as the bar diameter increases. This is due to the induced shear and effect of the anchor head. The shear caused by the tension in GFRP bars leads to a non-uniform stress distribution from the

outer surface of the bar toward its core. The induced stress has the lowest value at the core and the highest at the surface (due to higher interaction between concrete and the bar). Stress changes create more tensile stresses in smaller-diameter bars than in larger ones [34], resulting in a higher f_s/f_{ps} ratio of smaller bars than larger bars.

3.4.2 Influence of concrete compressive strength

To investigate the effect of concrete compressive strength on pullout behaviour between GFRP bar and concrete, two types of concrete whose compressive strengths were significantly different from each other (i.e. 20.4 MPa and 40.2 MPa) have been used. The compressive strength of concrete was an effective parameter in the pullout behaviour of both anchored and un-anchored GFRP reinforced concrete. Figure 8 shows the values of f_s/f_{ps} fsfpsfor different cases of the two concrete types. According to Fig. 8-a, the developed tensile stress of C2 specimens is significantly higher than those of specimens with C1 concrete. For instance, in anchor types IV, III, and II specimens with C2 concrete, the developed tensile stress increased by about 68, 41, and 14%, respectively, compared to reference samples. However, the presence of an anchor head in concrete type C1 has reduced the developed tensile stress by about 26, 30 and 37% for 12.7, 9.52 and 6.35 mm bars, respectively. The main reason for the such weak performance of the anchored sample is the low shear strength of concrete type C1,

**Fig. 7** Influence of bar diameter on GFRP bars' tensile stress developed
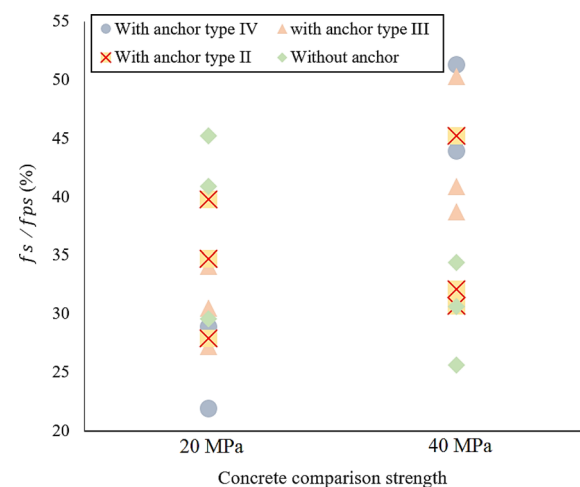
Fig. 8 Influence of concrete comparison strength on GFRP bars' tensile stress developed

resulting in early interface cracking between the concrete and the anchor and quick propagation of the developed crack to the concrete surface. On the other hand, in anchored specimens with C2 concrete type, concrete could carry much higher induced shear forces, thus, cracking and slip started at much higher applied loads. The tensile stress developed in concrete type C2 for 12.7, 9.52 and 6.35 mm bars has increased about 43, 55 and 61%, respectively, with respect to reference samples.

3.4.3 Influence of the anchor shape

Since the concrete compressive strength of C1 (i.e. 20.4 MPa) is inadequate, the anchorage system was found inefficient for such low-strength concrete. Therefore, only the anchorage shape effect of C2 specimens is compared. Figure 9 presents the influence of the anchor head types on the developed tensile stress (fs/fps) for C2 concrete and three different GFRP bar diameters. As is seen, type IV specimens have the highest ratio compared to the other types, which can be attributed to the less stress concentration and higher mechanical interlocking between the anchored bar and the concrete. This can also be confirmed by comparing types III and II. In type III anchors, the higher pullout strength resulted from increased mechanical interaction between the anchor and the concrete compared to type II.
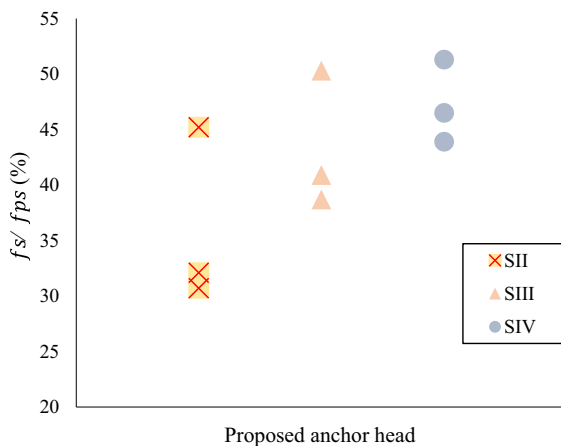
Fig. 9 Influence of proposed anchor head type on the tensile stress developed

3.5 Prediction of the pullout bearing capacity

In this section, considering the effects of various parameters such as bar diameter and compressive strength of the concrete on the bar developed tensile stress, an equation to predict the pull-out bearing capacity has been derived. Since the anchor heads were not efficient in low-strength concrete (e.g. 20.4 MPa), only specimens with concrete compressive strength of 40.2 MPa have been considered. Using non-linear regression analysis, the pull-out bearing capacity of straight GFRP bars can be calculated from Eq. (1) for specimens with $f'_c \geq 40 MPa$.

$$f_s = 0.1507 f_{ps} \left(\frac{\sqrt{f'_c} \times l_d \times C}{d_b^2} \right)^{0.1031} \tag{1}$$

where,

d_b= bar diameter (mm)

C= the lesser of the cover to the center of the bar (mm)

f'_c= concrete compressive strength (MPa)

l_d= the development (bond) length (mm)

f_{ps}= tensile strength capacity of the bar (kN)

In addition, three equations related to tensile stress are introduced for all types of proposed anchors in order to quantify the contribution of the different anchor heads to the pull-out behaviour of the specimens. The pull-out bearing capacity of the GFRP bars with the anchors is expressed in Eqs. (2) to (4), which is basically the sum of straight bar contribution (i.e. Equation (1)) and the tensile capacity contribution of the anchor heads.

$$f_s = f_{ps} \left(0.1507 \left(\frac{\sqrt{f'_c} \times l_d \times C}{d_b^2} \right)^{0.1031} + 0.0612 \left(e^{0.0014 \left(\frac{\sqrt{f'_c} \times l_d \times C}{d_b^2} \right)} \right) \right) \quad \text{for SII} \tag{2}$$

$$f_s = f_{ps} \left(0.1507 \left(\frac{\sqrt{f'_c} \times l_d \times C}{d_b^2} \right)^{0.1031} + 0.1059 \left(e^{0.0003 \left(\frac{\sqrt{f'_c} \times l_d \times C}{d_b^2} \right)} \right) \right) \quad \text{for SIII} \tag{3}$$

$$f_s = f_{ps} \left(0.1507 \left(\frac{\sqrt{f'_c} \times l_d \times C}{d_b^2} \right)^{0.1031} + 0.1727 \left(e^{0.0001 \left(\frac{\sqrt{f'_c} \times l_d \times C}{d_b^2} \right)} \right) \right) \quad \text{for SIV} \tag{4}$$

Table 6 Predicted versus experimental pull-out test results

Specimen	Predicted f_s/f_{ps}	Experimental f_s/f_{ps}	Error (%)
C2-SI-D2	0.32	0.34	7.63
C2-SII-D2	0.42	0.45	6.96
C2-SIII-D2	0.45	0.50	10.96
C2-SIV-D2	0.47	0.51	8.74
C2-SI-D3	0.29	0.26	11.48
C2-SII-D3	0.35	0.31	12.93
C2-SIII-D3	0.41	0.39	5.86
C2-SIV-D3	0.44	0.45	1.34
C2-SI-D4	0.27	0.31	15.03
C2-SII-D4	0.33	0.32	1.24
C2-SIII-D4	0.39	0.41	5.66
C2-SIV-D4	0.43	0.44	3.10

Table 6 summarises the predicted and experimental values for f_s/f_{ps}. As is seen, the predicted values are in good agreement with the test results (i.e. maximum Error of 15%).

3.6 ANOVA (analysis of variance)

In order to quantify each variable's contribution to the developed tensile stress ratio, f_s/f_{ps}, of different specimens tested in this study, a two-way analysis of variance (ANOVA) with repetition, including the three identical sample results for each condition, was performed. Tables 7 and 8 summarise the ANOVA results for 20.4 MPa and 40.2 MPa concrete types, based on (i) bar size (i.e. #2, #3, and #4) and anchorage shape (i.e. Type I, Type II, Type III, and Type IV). In Tables 7 and 8, SS denotes the sum of squares of the experiment results' deviations from their mean. The degrees of freedom associated with the sample variance are denoted by df. The mean square (the sum of squares divided by the degrees of freedom) is MS; F is the variation among the sample means divided by the variation within the samples; *P*-value represents the probability that calculated F happens within the assumption of the null hypothesis; F_{crit} in the equivalent of p-value = 0.05 and represents the significance of each parameter on the final output (i.e., if $F_{crit} < F$, the parameter is effective and has a considerable effect on the final output).

As is seen in Tables 7 and 8, both p-values related to bar size and anchorage shape are smaller than 0.05 (i.e. $F_{crit} < F$). Therefore, it is concluded that for both 20.4 MPa and 40.2 MPa, concrete compressive strength, anchorage shape, and bar diameter are effective factors in the bond strength behaviour of GFRP-reinforced concrete specimens.

Moreover, by comparing the contribution of each factor in Table 7 with those in Table 8, one can conclude that the effect of anchorage shape becomes higher when using higher strength concrete (i.e. 64% in 40.2 MPa specimens compared to 49% in 20.4 MPa specimens). This confirms the previous fact that if an appropriate concrete compressive strength is used, the optimized anchorage shape could further improve the bond quality of GFRP-reinforced concrete.

Table 7 Two-way ANOVA results for 20.4 MPa concrete

Source of variation	SS	df	MS	F	*P*-value	F_{crit}	Contribution (%)
Anchor shape	242.017	3.000	80.672	14.933	0.003	4.757	48.688
Bar size	222.647	2.000	111.323	20.607	0.002	5.143	44.791
Error	32.413	6.000	5.402				6.521
Total	497.077	11.000					100

Table 8 Two-way ANOVA results for 40.2 MPa concrete

Source of variation	SS	df	MS	F	P-value	F_{crit}	Contribution (%)
Anchor shape	492.630	3.000	164.210	29.442	0.001	4.757	64.170
Bar size	241.595	2.000	120.798	21.658	0.002	5.143	31.470
Error	33.465	6.000	5.578				4.359
Total	767.690	11.000					100

4 Conclusions

To study the efficiency of an innovative anchorage system, the current research has experimentally tested 72 pullout specimens. The experimental variables include the configuration of the anchorage system, the bar diameter, and the concrete compressive strength. Based on the obtained results, the following conclusions were obtained:

- Using glass-fibre anchor heads to enhance the bond between GFRP bars and concrete with a compressive strength of 40.2 MPa is efficient. Optimizing the shape of the anchor allowing for additional mechanical interlocking and friction with the concrete, further improves the bond performance.
- The shape of the anchorage system and the concrete compressive strength affect the pullout failure mode. Non-anchored specimens fail in pullout failure (no crack propagation toward the concrete surface), while anchored specimens fail in concrete splitting. Furthermore, in low-strength concrete specimens (e.g. 20.4 MPa), pull-out failure is due to the concrete crushing, while in high-strength specimens, it is due to the GFRP bar surface peeling-off.
- Concrete compressive strength is found to be a significant factor in determining the efficiency of the anchorage system. Due to the low shear strength and lack of confinement strength, the anchorage system reduces the developed tensile stress of the GFRP bar embedded in low-strength concretes (e.g. 20.4 MPa). However, if the concrete has appropriate compressive strength (e.g. 40.2 MPa), the developed tensile stress could increase up to 68% depending on the anchorage system used.
- The shape of the anchor head is found to be a key parameter in the bond performance of anchored GFRP bars embedded in concrete. The ancho system with gradually changing the cross-section (i.e. largest diameter at the end and smallest at the top) is the most efficient type. In contrast, the anchorage with a constant cross-section is the least efficient system.

Declarations

Competing interest The authors declare that they have no known competing financial interests or personal relationships that could have appeared to influence the work reported in this paper.

References

1. ACI (American Concrete Institute) (2015) "Guide for the design and construction of concrete reinforced with FRP bars." ACI 440–1R, Farmington Hills, MI.
2. Doostmohamadi A, Karamloo M, Oskouei AV, Shakiba M, Kheyroddin A (2022) Enhancement of punching strength in GFRP reinforced single footings by means of handmade GFRP shear bands. Eng Struct 262:114349
3. Sharifianjazi F, Zeydi P, Bazli M, Esmaeilkhanian A, Rahmani R, Bazli L, Khaksar S (2022) Fibre-reinforced polymer reinforced concrete members under elevated

temperatures: a review on structural performance. Polymers 14(3):472

4. Luck JD, Bazli M, Rajabipour A (2022) Bond between fibre-reinforced polymer tubes and sea water sea sand concrete: mechanisms and effective parameters: critical overview and discussion. Fibers 10(1):8

5. Antonietta Aiello M, Leone M, Pecce M (2007) Bond performances of FRP rebars-reinforced concrete. J Mater Civ Eng 19(3):205–213

6. Hosseini SM, Shakiba M, Bazli M, Javaheri A (2022) Using four-point flexure test to investigate effects of temperature and bar size on the tensile properties of GFRP bars. Polym Test 112:107627

7. Bazli M, Heitzmann M, Hernandez BV (2022) Durability of Fibre-reinforced polymer-wood composite members: an overview. Compos Struct 295:115827

8. Hao Q-D, Wang Y-L, Zhang Z-C, Ou J-P (2007) Bond strength improvement of GFRP rebars with different rib geometries. J Zhejiang Univ Sci A 8(9):1356–1365

9. Feng P, Wang J, Wang Y, Loughery D, Niu D (2014) Effects of corrosive environments on properties of pultruded GFRP plates. Compos B Eng 67:427–433

10. Najafabadi EP, Bazli M, Ashrafi H, Oskouei AV (2018) Effect of applied stress and bar characteristics on the short-term creep behavior of FRP bars. Constr Build Mater 171:960–968

11. Bazli M, Heitzmann M, Hernandez BV (2021) Hybrid fibre reinforced polymer and seawater sea sand concrete structures: a systematic review on short-term and long-term structural performance. Constr Build Mater 301:124335

12. Bazli M, Ashrafi H, Oskouei AV (2017) Experiments and probabilistic models of bond strength between GFRP bar and different types of concrete under aggressive environments. Constr Build Mater 148:429–443

13. Oskouei AV, Kivi MP, Araghi H, Bazli M (2017) Experimental study of the punching behavior of GFRP reinforced lightweight concrete footing. Mater Struct 50(6):1–14

14. Shakiba M, Bazli M, Karamloo M, Mohammad Reza Mortazavi S (2022) Bond-slip performance of GFRP and steel reinforced beams under wet-dry and freeze-thaw cycles: the effect of concrete type. Constr Build Mater 342:127916

15. Bazli M, Zhao X-L, Jafari A, Ashrafi H, Raman RS, Bai Y, Khezrzadeh H (2021) Durability of glass-fibre-reinforced polymer composites under seawater and sea-sand concrete coupled with harsh outdoor environments. Adv Struct Eng 24(6):1090–1109

16. Chun SC, Lee SH, Kang TH, Oh B, Wallace JW (2007) Mechanical anchorage in exterior beam-column joints subjected to cyclic loading. ACI Struct J 104(1):102

17. Lee H-J, Yu S-Y (2009) Cyclic response of exterior beam-column joints with different anchorage methods. ACI Struct J 106(3):329

18. Wallace JW, McConnell SW, Gupta P, Cote PA (1998) Use of headed reinforcement in beam-column joints subjected to earthquake loads. Struct J 95(5):590–606

19. Islam S, Afefy HM, Sennah K, Azimi H (2015) Bond characteristics of straight-and headed-end, ribbed-surface, GFRP bars embedded in high-strength concrete. Constr Build Mater 83:283–298

20. Xiong Z, Wei W, Liu F, Cui C, Li L, Zou R, Zeng Y (2021) Bond behaviour of recycled aggregate concrete with basalt fibre-reinforced polymer bars. Compos Struct 256:113078

21. Tighiouart B, Benmokrane B, Gao D (1998) Investigation of bond in concrete member with fibre reinforced polymer (FRP) bars. Constr Build Mater 12(8):453–462

22. Kazemi H, Yekrangnia M, Shakiba M, Bazli M, Oskouei AV (2022) Bond-slip behaviour between GFRP/steel bars and seawater concrete after exposure to environmental conditions. Eng Struct 268:114796

23. Pecce M, Manfredi G, Realfonzo R, Cosenza E (2001) Experimental and analytical evaluation of bond properties of GFRP bars. J Mater Civ Eng 13(4):282–290

24. Zou R, Liu F, Xiong Z, He S, Li L, Wei W (2021) Experimental study on fatigue bond behaviour between basalt fibre-reinforced polymer bars and recycled aggregate concrete. Constr Build Mater 270:121399

25. Xiong Z, Zeng Y, Li L, Kwan A, He S (2021) Experimental study on the effects of glass fibres and expansive agent on the bond behaviour of glass/basalt FRP bars in seawater sea-sand concrete. Constr Build Mater 274:122100

26. E. Cosenza (1996) Bond characteristics and anchorage length of FRP rebars. In: Proc. 2nd Int. Conf. on Advanced Compos. Mat. In Bridge Struct., M. El-Badry, 1996.

27. Hasaballa MH, El-Ragaby A, El-Salakawy EF (2011) Seismic performance of exterior beam–column joints reinforced with glass fibre reinforced polymer bars and stirrups. Can J Civ Eng 38(10):1092–1102

28. Mohamed HM, Benmokrane B (2012) Pullout capacity behaviour of FRP-headed rebars. In: Proceedings of the 5 th International Conference on Composites in Civil Engineering, Rome, Italy, pp 13–15.

29. Ahmed EA, El-Sayed AK, El-Salakawy E, Benmokrane B (2010) Bend strength of FRP stirrups: comparison and evaluation of testing methods. J Compos Constr 14(1):3–10

30. Shakiba M, Oskouei AV, Karamloo M, Doostmohamadi A (2021) Effect of mat anchorage on flexural bonding strength between concrete and sand coated GFRP bars. Compos Struct 273:114339

31. Ashrafi H, Bazli M, Oskouei AV (2017) Enhancement of bond characteristics of ribbed-surface GFRP bars with concrete by using carbon fiber mat anchorage. Constr Build Mater 134:507–519

32. Elsayed TA, Eldaly A, El-Hefnawy A, Ghanem G (2011) Behaviour of concrete beams reinforced with hybrid fiber reinforced bars. Adv Compos Mater 20(3):245–259

33. Khederzadeh H, Sennah K (2013) Pullout strength of pre-installed GFRP bars in concrete. In: CSCE 2013 General Conference. Quebec, Canada2013, pp 1-9

34. Maranan GB, Manalo AC, Karunasena W, Benmokrane B (2015) Pullout behaviour of GFRP bars with anchor head in geopolymer concrete. Compos Struct 132:1113–1121

35. Benmokrane B, Mohamed HM, Manalo A, Cousin P (2017) Evaluation of physical and durability characteristics of new headed glass fiber–reinforced polymer bars for concrete structures. J Compos Constr 21(2):04016081

36. Zhang B, Zhu H, Wu G, Wang Q, Li T (2020) Improvement of bond performance between concrete and CFRP bars with optimized additional aluminum ribs anchorage. Constr Build Mater 241:118012

37. Tebeta R, Fattahi A, Ahmed N (2020) Experimental and numerical study on HDPE/SWCNT nanocomposite elastic properties considering the processing techniques effect. Microsyst Technol 26(8):2423–2441
38. ACI Committee 211.1–91 (2000) Standard practice for selecting proportions for normal, heavyweight, and mass concrete. In: ACI manual of concrete practice, Part 1. Michigan (USA): American Concrete Institute. p 38.
39. ASTM C39 / C39M (2021) Standard test method for compressive strength of cylindrical concrete specimens. West Conshohocken, USA.
40. Design CSA (2012) Construction of Building Structures with Fibre-Reinforced Polymers (CAN/CSA8061 S–S2). In: Canadian Standards Association: Mississauga, ON, Canada.